Electronic Supporting Information (ESI)

HKUST-1 Nano-Metal-Organic Frameworks Combined with $ZnGa_2O_4$: Cr^{3+} Near-Infrared Persistent Luminescence Nanoparticles for Vivo Imaging and Tumor Chemodynamic&Photothermal Synergic Therapy

Bin Yu[a], Yun-Jian Wang[a], Yuan-Ying Lin[a], Yan Feng[a], Juan Wu[d], Wei-Sheng Liu[a*], Min Wang[b*], Xiu-Ping Gao[c*]

[a]The Key Laboratory of Nonferrous Metal Chemistry and Resources Utilization of Gansu Province and State Key Laboratory of Applied Organic Chemistry, College of Chemistry and Chemical Engineering, Lanzhou University, Lanzhou730000, China.

[b]School of Basic Medical Sciences, Lanzhou University, Lanzhou730000, China.

[c]School of Physical Science and Technology. Lanzhou University, Lanzhou730000, China.

[d]The Key Laboratory of Rare Earth Functional Materials and Applications, International Joint Research Laboratory for Biomedical Nanomaterials of Henan, Zhoukou Normal University, Zhoukou 466001, China

* Corresponding authors. Tel: +86 931 8915151; fax: +86 931 8912582

.E-mail addresses: liuws@lzu.edu.cn (W. S. Liu)

I. EXPERIMENTAL SECTION

(A) Materials

Metal nitrate pentahydrate ($Zn(NO_3)_2·6H_2O$, $Ga(NO_3)_3·H_2O$, $Cr(NO_3)_3·9H_2O$, >99.9%), $CuCl_2·2H_2O$ (AR), hexadecyl trimethyl ammonium bromide (CTAB, >99%) and $Na_2S·9H_2O$ (>98%) were all purchased from Meryer chemical technology Co., Ltd (Shanghai). Diethanolamine (99%), 1,3,5-Benzenetricarboxylic acid (H_3BTC, >98%) and tetraethyl orthosilicate (TEOS, >99%) were bought from Aladdin Bio-Chem technology Co., Ltd (Shanghai). The cell counting kit 8 (CCK8), 4', 6-diamidino-2-phenylindole (DAPI) and reactive oxygen species assay kit (ROS assay kit, DCFH-DA) were bought from Beyotime biotechnology (Shanghai, China). RPMI 1640 and fetal bovine serum (FBS) were purchased from Hyclone Corporation (USA) and the BI

Corporation (Israel). Paraformaldehyde was bought from the Tianjin Kaixin chemical industry (China).

(B) Preparation of mesoporous SiO_2

The mesoporous SiO_2 （$mSiO_2$）was synthesized according to the previous literature[1]. Firstly, Ethanol (22.5 mL) and CTAB (25%, 20.8 mL) aqueous solution were mixed in 150 mL ultrapure water by sonication. Diethanolamine was added into the mixed solution with stirring under 60 ℃ for 3 h. And then, the white suspension was gradually formed after TEOS (14 mL) was slowly added into the mixed solution. The mixture was kept stirring for 4 h and cooled down to room temperature. The white product was collected by centrifugation and washed with water and ethanol sequentially to obtain $mSiO_2$.

(C) Synthesis of $mSiO_2@Zn_{1.05}Ga_{1.9}O_4$: Cr (SZGO) nanoparticles

$mSiO_2@Zn_{1.05}Ga_{1.9}O_4$: Cr (SZGO) nanoparticle was synthesized via calcination to combinate the persistent luminescence particles loaded with silica balls. Firstly, Zn $(NO_3)_2$, Ga $(NO_3)_3$, and Cr $(NO_3)_2$ were mixed with a certain ratio of 1.1:1.9:0.005 in a centrifuge tube contained 1 mL ultrapure water/ethanol solution. And then, 100 mg $mSiO_2$ was added in to the transparent solution to obtain a colloidal mixture. The mixture was mixed well by sonication, and then dried in oven for 6h to obtained the powder solids. Finally, the production was transferred to the muffle furnace and calcined at 800 °C for 3 h (5 °C/min).

(D) Synthesis of $mSiO_2@Zn_{1.05}Ga_{1.9}O_4$: Cr (@HKUST-1 (HSZGO) and $mSiO_2$@HKUST

HSZGO was synthesized according to the previously published literature[2] with slight modification. Briefly, $CuCl_2$ (1.5 mmol) and H_3BTC (0.83 mmol) were dissolved in ultrapure water and ethanol, respectively. And then, SZGO nanoparticles were dispersed in the $CuCl_2$ aqueous solution with vigorously stirring for 1h as the preparation solution. The preparation solution was mixed with H_3BTC ethanol solution in a round-bottomed flask, and transferred to the Teflon liner. After stirred for 0.5 h, the mixture system was placed in an autoclave and moved into the muffle furnace at 120 ℃ overnight. The sediment was purified with ultrapure water and ethanol, followed by kept in a muffle furnace at 150 ℃ overnight.

For comparison, $mSiO_2$@HKUST-1 was synthesized by using the same method as above, which replaced SZGO nanoparticles with $mSiO_2$.

(E) Characterization

(F) The powder X-ray diffraction (PXRD) pattern was recorded on a Rigaku-DMax 2400 X-ray diffractometer under CuKα radiation. Fourier transform infrared (FT-IR) spectrum was obtained from a Bruker Vertex 70 infrared spectrometer with the KBr pellet technique. UV-Vis absorption spectrum was recorded by a Varian Cary 5000 UV-Vis-NIR spectrophotometer. The morphology and microstructure were obtained through a scanning electron microscopy (SEM, Apreo S) and transmission electron microscopy (TEM, Tecnai F30, 300kV). X-ray photoelectron spectroscopy (XPS) was measured by a Kratos AXIS Ultra DLD (Kratos). Thermogravimetric analysis (TGA) was recorded on a TGA PT1600 (Linseis) (10 °C/min). The Brunauer−Emmett−Teller (BET) and Barrett–Joyner–Halenda (BJH) analysis was measured by an ASAP2020M&TriStar3020 (Micromeritics instrument Corp) automatic specific surface area physical adsorption instrument. Steady-state photoluminescence (PL) spectra were collected through a Horiba FL-3 (HORIBA Instruments Incorporated) fluorescence spectrophotometer. An LMT-photometer B520 (Germany) was used to monitor the afterglow decay time solid samples. And the camera images of afterglow luminescence were obtained by using a pco. edge 4.2 sCMOS camera. The real-time temperature changes were recorded by a Fluke TiS10 infrared camera 9 Hz (Fluke). Confocal laser scanning microscope (CLSM) image was monitored from an inverted fluorescence microscope (Olympus FV3000, Tokyo). Thermal images of mice were obtained via a FLIR E95

thermal infrared imager. Histological analysis images were taken by a biological microscope (EX30LED, Shunyu). The content of Cu in major organ tissues and tumors were measured by an inductively coupled plasma mass spectrometer (ICP-MS) (iCAPQc, Thermo Electron Corporation). The persistent luminescence (PersL) images were obtained by an IVIS Lumina II system.TGA

The mass ratio of HKUST-1 and SZGO was calculated as follows: It is assumed that the mass proportion of HKUST -1 and SZGO in HSZGO is x and y. After heating to 800℃, the mass loss of HKUST-1 and SZGO are 77.03% and 4.05%, respectively, so the mass loss of HSZGO should be 77.03%*x+4.05%*y. While it was known that the final mass loss of HSZGO is 54.403%, and x+ y =1, it can be calculated that x is 0.69 and y is 0.31. So, the value of $m_{HKUST-1}$: m_{SZGO} is 1:0.45.

(G) Photoluminescence (PL) and decay time measurements

The PL spectrum of solid samples were recorded with the excitation optical source of 254 nm. The decay time of powers was measured after the excitation of 254 nm UV lamp for 10 min or 650 nm lamp for 3min. While the lamp was closed, the measurements began to record immediately.

The decay time of solution samples were obtained by removing the light source after charged with a 254 nm lamp and 650 nm LED for 10min and 3 min. A steady-state photoluminescence spectrum was used to monitor the intensity of the emission peak at 696 nm.

(H) Photothermal effects of HSZGO aqueous solution in the presence of NaHS in vitro

The solution of HSZGO aqueous solution at different concentrations (0, 0.125, 0.25, 0.375, 0.5, 0.75, 1 mg/mL) in the presence of NaHS at different concentrations (0, 0.25, 0.5, 1.25, 2.5, 5 mM), were exposed under the different powers of an 808 laser (0.25, 0.5, 0.8, 1, 1.25, 1.5, 1.75, 2 W/cm^2). The real-time temperature changes of solution which under different pH (7.4, 6.5, 6.0, 5.0) and mixed with interfering materials (2.5 mM GSH, 1.7 mg/mL BSA, L-cysteine, H_2O_2,) were recorded to evaluate the influence under 808 nm irradiation of 2 W/cm^2.

(I) Photothermal conversion efficiency

The photothermal conversion efficiency (***η***) of HSZGO nanoparticles was calculated according to the method reported in the preview literature[3, 4]. The aqueous solution (2 mL) contained HSZGO (1 mg/ mL) and NaHS (5 mM) was exposed to a continuous irradiation of 808nm (2 W/cm^2) laser. Then turned off the laser and let the solution cooled naturally to close to the environment temperature. The temperature change of solution is recorded every 30s. The **η** is calculated by the following formula:

$$\eta = \frac{hS\left(T_{max} - T_{surr}\right) - Q_S}{I\left(1 - 10^{-A_\lambda}\right)} \times \mathbf{100\%} \qquad \mathbf{(1)}$$

From the recorded data, the maximum steady temperature (**T_{max}**) and the environmental temperature (**T_{Surr}**) are 60.5℃ and 24.8℃. The laser power density (**I**) was 2 W/cm^2. and the absorbance of the solution at 808 nm (**A_λ**) was 0.703. Qs is heat dissipated from light absorbed by a quartz container containing ultrapure water without sample. hs was

calculated as followed:

$$\mathbf{hS} = \frac{m_D * C_D}{\tau_s} \times \mathbf{1000} \qquad \mathbf{(2)}$$

h represents the heat transfer coefficient, **S** denotes the surface area of the container. Furthermore, the mass of sample ($\mathbf{m_D}$) and $\mathbf{C_D}$ is 2 g and 4.2 J/g·℃. Thus, only the $\boldsymbol{\tau_s}$ is unknown.

the sample system time constant ($\boldsymbol{\tau_s}$), which calculated as Eq.3:

$$\boldsymbol{\tau_s} = \frac{t}{-ln(\theta)} \qquad (\mathbf{3})$$

And linear time data versus -lnθ is from the cooling period as followed:

$$\boldsymbol{\theta} = \frac{T - T_{Surr}}{T_{max} - T_{Surr}} \qquad \mathbf{(4)}$$

According to the Eq.3 ad Eq.4, $\boldsymbol{\tau_s}$ **was** calculated to be 300.375s. According to Eq.2, hS was equaled to 27.96 mW/℃. And Qs was calculated to be 56.596 mW. Thus, the according to photothermal conversion efficiency can be calculated as 58.7%.

(J) Generation of ·OH in vitro

3,3',5,5'-Tetramethylbenzidine (TMB) (500 μg/mL) was used to confirm the generation of ·OH in HSZGO (500 μg/mL) solution in the presence of H_2O_2 with different concentration (0, 25, 50, 125, 250 μM). The only H_2O_2 and only HSZGO groups were prepared for comparison to prove the generation of ·OH in the HSZGO (500 μg/mL) aqueous solution added with H_2O_2. After vibrating for 12h, the UV-Vis absorption spectra of solutions were measured to compare the characteristic absorption peaks changes of TMB.

(K) Cell culture, endocytosis and viability assays

Human gastric mucosal epithelial cell lines (GES-1 cells), hepatoma 22 cell lines (H22 cells), human hepatocellular carcinomas cell lines (HepG2 cells) were all acquired from the Shanghai Institute of Biology. The cell lines were incubated in RPMI-1640 medium, contained 10% heat-inactivated FBS, penicillin and streptomycin. The culture mediums should be replaced daily. All of the cells were cultured in culture flasks at 37 ℃ with 5% CO_2.

H22 cells were seeded in 96-well plates overnight and incubated with HSZGO (50 ug/mL) for different times (30 min, 4 h) in order to monitor the uptake of HSZGO by tumor cells. The cells were washed with PBS and fixated with 4% paraformaldehyde solution, and then stained with DAPI. Finally, the cells were put onto an inverted microscope to take fluorescent photographs under the irradiation of 405 nm.

The CCK-8 assay was applied to assess the cell viability. GES-1, H22, and HepG2 cells were growth in 96-well plates for 24 h. The cells were treated with PBS and HSZGO PBS solutions with different concentrations (0.3125, 0.625, 1.25, 2.5, 5, 10, 20 ug/mL), respectively, and incubated for another 4 h and 6 h in the CO_2 incubator at 37 °C. There are six parallel wells were experimented for each particular concentration group. And then, after added with 10 μL CCK-8 into each well, all of the cells were continuously cultured in a cell incubator for 4 h. Finally, the absorbance (Abs) of samples at 450 nm were measured to calculated the cell viability by the following formula.

Cell viability (%) = $(Abs_{sample} / Abs_{control}) \times 100\%$

Abs_{sample} and $Abs_{control}$ are stand for the Abs of the sample with and without HSZGO, respectively.

(L) In vitro antitumor effect

GES-1, H22, and HepG2 cells were seeded in 96-well plates overnight and divided into four groups for experiment，respectively : a) without treatment; b) cells irradiated with 808 nm laser; c) cells incubated with HSZGO; d) cells incubated with HSZGO and irradiated with 808 nm laser. There are six parallel wells were experimented for each group. After incubated with HSZGO for 4h, the groups of b, d were irradiated with 808nm ($2W/cm^2$) for 15min. And then, all of the cells were continuously cultured after added with CCK-8 (10 μL) for 4 h, and measured the absorbance (Abs) of samples at 450 nm to calculated the cell viability.

(M) Intracellular ·OH generation

DCFH-DA testing kit was used to verify the formation of ·OH in tumor cells in the presence of HSZGO. The HepG2 cells were growth in 96-well plates overnight, and then respectively cultured with: a) PBS (pH=7.4), b) H_2O_2, c) HSZGO, d) HSZGO + H_2O_2. And then, the cells were incubated for another 4 h. All of the cells were washed with PBS solution and further cultured with DCFH-DA for 20 min. Finally, the cells were taken fluorescence images by CLSM to measure the generation of intracellular ·OH.

(N) In vivo NIR PersL imaging

HSZGO (12 mg/mL, 100 μL) PBS solution which pre-excited by 254 nm UV lamp for 10 min was in situ injected into the mice. And then, the mice were taken for the NIR

PersL imaging via IVIS II Lumina system at different time points. Furthermore, those mice were recharged with LED for 3 min and the PersL signals were captured again to verify the rechargeable imaging ability of HSZGO in vivo.

(O) Biodistribution analysis

After intraperitoneal injected with HSZGO for 6 h, The H22 tumor-bearing mice were euthanized, and dissected the major organs (heart, liver, spleen, lung, kidney) and tumors. Then, these tissues and tumors were collected to irradiate under a 254 nm lamp for 5 min and toke images by the IVIS II Lumia system.

In addition, the biodistribution of HSZGO was evaluated by ICP-MS measurements. The tumor-bearing mice were sacrificed to dissect the major organs and tumors after injected intraperitoneally with 100 μL HSZGO (20 mg/kg) for 24 h. And the major organs and tumors were digested with aqua regia to experiment the ICP-MS measurements. In order to assess the detention time of HSZGO in tumors, the tumor-bearing mice were carried out euthanasia after injected with HSZGO for 0.5, 6, 12, 24, 48h, respectively. And the tumors were collected to digest with aqua regia for ICP-MS measurements.

The biodistribution of HSZGO in the major organs at different times was studied by heathy female KM mouse. After intraperitoneal injection of HSZGO (20 mg/kg), the mice were dissected at varying times (0, 1 h, 1 d, 3 d, 5 d, 7 d, 10 d) and collected the major organs. The major organs were weighted and digested with aqua regia to experimented the ICP-MS measurements.

(P) Animals experiments and histological staining

All of the animal experiment programmer and implementation have been approved and guided by the Ethics Committee of the Basic Medical School, Lanzhou University. Female KM mice which weighed approximately 18~20 g (4~6weeks) were purchased from the Animal Experiment Center of Lanzhou University and fed for one week. And then, those mice were subcutaneous implanted with H22 tumor cells ($3.5*10^5$/100μL/site) under the right oxter to established the tumor-bearing mouse model.

When the tumors size of H22 tumor-bearing mice achieved to an average value of about 50~100 mm^3, the mice were randomly divided into five groups (n=10/group): (A)injected with saline (100 μL); (B) injected with saline (100 μL)+ 808 nm laser (2W/cm^2, 3min); (C) injected with HSZGO (20 mg/kg,100 μL); (D) injected with HSZGO (20 mg/kg, 100 μL) +808 nm laser (2W/cm^2, 3min); (E) injected with S-adenosyl-l-methionine (SAM,40 mg/kg,100 μL) + HSZGO (20 mg/kg, 100 μL) + 808nm laser(2W/cm^2, 3min). The SAM, which is injected 12h before injected with HSZGO, can activate the overexpressed cystathionine β-synthase (CBS, which is one of the catalytic enzymes for the generation of H_2S in cells) in tumor cells to catalyze the formation of H_2S from L-cysteine. The tumor-bearing mice were experimented with different treatment once every seven days. Saline and saline +808nm laser groups were selected as control groups to compared with the other treatment groups. And those groups can also verify the influence of 808nm laser for tumor treatment. The group injected with HSZGO was used to evaluate the effects of chemodynamic therapy

(CDT). At last, the groups of HSZGO+808nm laser (2 W/cm^2, for 3 min) and SAM+ HSZGO+808nm laser (2 W/cm^2, for 3 min) were experimented to demonstrate the efficacy of synergistic therapy. The tumor size was surveyed daily with a digital caliper. And the volume of tumors was obtained according to the following formula: V=length×width^2/2. The relative tumor volume is calculated by V/V_0(V_0 is the untreated initial tumor volume). During the experiment, the body weight of tumor-bearing mice was recorded daily by using a laboratory balance, in order to obtain the relative body weight. And finally, after all of the mice were euthanized, the tumor was dissected and record its size. H&E and TUNEL staining of tumors were proceed after paraffin embedded to observe the cell apoptosis of tumor cells.

(Q) Biosecurity assessment

The major organs were dissected from experimented mice and fixated in 4% formaldehyde overnight. After that, these major organs were sectioned into slices, embed in paraffin, stained with H&E and took images via an optical microscope for histological analysis, in order to evaluate the biosafety of HSZGO.

(R) Thermal imaging

The H22 tumor-bearing mice were randomly divided into three groups: (A)injected with saline (100 μL); (B) injected with HSZGO (20 mg/kg,100 μL); (C) injected with SAM (40 mg/kg,100 μL) + HSZGO (20 mg/kg,100 μL). After 6 h injection, the tumor sites were exposed to the irradiation of 808 nm laser (2 W/cm^2) for 3min. Then the temperature variation of tumor was recorded by a FLIR E95

thermal infrared imager.

(S) Statistical analysis

All experimental data in this study were processed and analyzed by using the GraphPad Prism 8.0 and Origin 9.0 software. The statistical significance was tested by one-way and two-way ANOVA statistical analysis.

Ⅱ. CHARACTERISATION

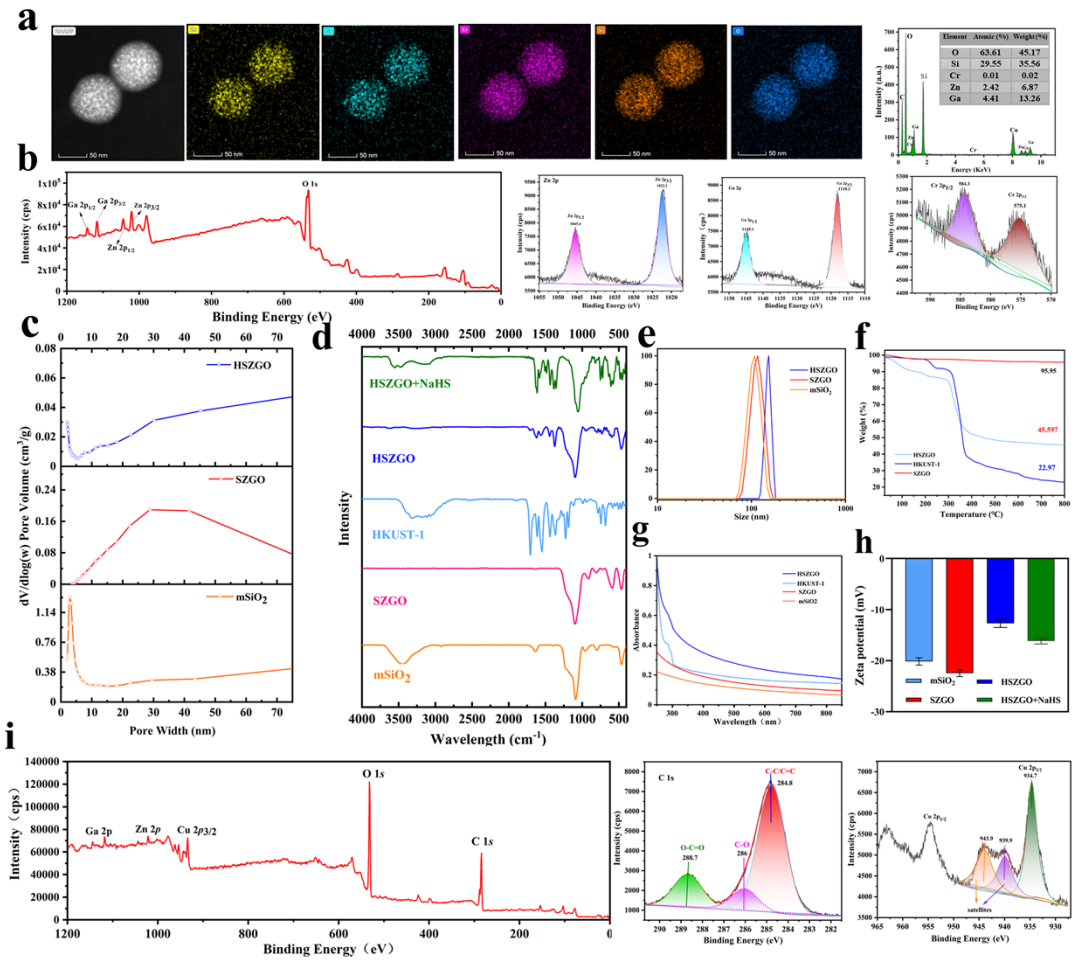

Figure S1. (a) EDS of SZGO nanoparticles. (b) XPS spectra and deconvoluted XPS peaks of SZGO. Typical wide survey and high resolution XPS spectra of Ga 2p, Zn 2p and Cr 2p. (c) Corresponding pore size distributions of $mSiO_2$, SZGO and HSZGO. (d) FT-IR spectra of $mSiO_2$, SZGO, HKUST-1, HSZGO and HSZGO+NaHS. (e) DLS characterization of $mSiO_2$, SZGO and HSZGO. (f) TGA results of SZGO, HKUST-1 and HSZGO. (g)The UV-Vis absorption spectra of $mSiO_2$, SZGO, HKUST-1 and

HSZGO. (h) Surface zeta potential of $mSiO_2$, SZGO, HSZGO and HSZGO+NaHS. The error bars represent standard errors (n=3). (i) The XPS spectra and deconvoluted XPS peaks of HSZGO. Typical wide survey, and high resolution XPS spectrum of C 1s and Cu 2p. (h)

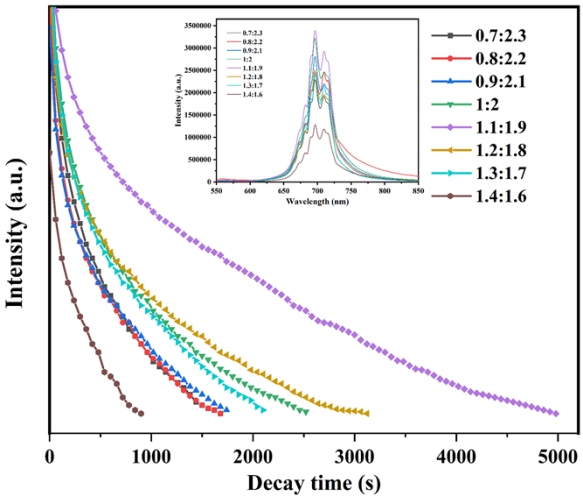

Figure S2. The emission spectra and decay times of $Zn_{1+x}Ga_{(2-x)}O_4$:Cr (x=-0.3~0.4) after excited with 254 nm excitation source.

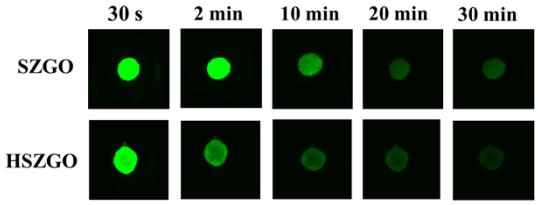

Figure S3. CCD camera imaging for afterglow luminescence of SZGO charged by 254 nm lamp.

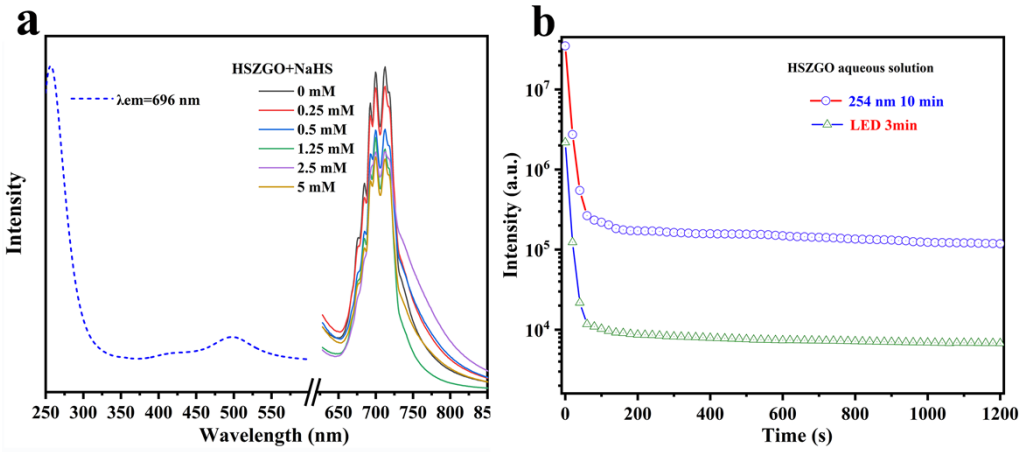

Figure S4. (a) The excitation of HSZGO aqueous solution and the emission spectra of HSZGO aqueous solution after added with different concentrations of NaHS. (b) NIR decay time of HSZGO solution at 696 nm after 10 min of 254 nm irradiation and 3 min of LED irradiation as a function of time recorded by fluorescence spectrophotometer.

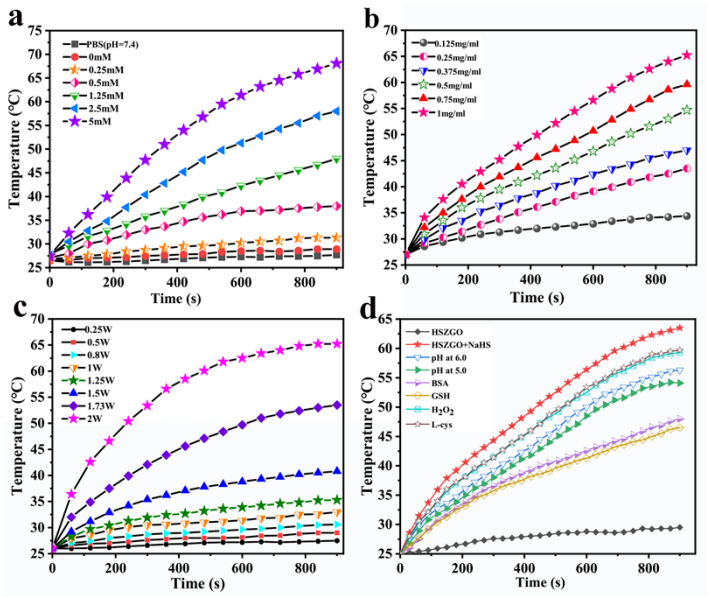

Figure S5. (a) Photothermal curves of HSZGO aqueous solution in different concentration of NaHS under 808 nm laser (2 W/cm^2) irradiation. (b) Photothermal curves of different concentration of HSZGO aqueous solutions in the presence of NaHS (5 mM) under 808 nm laser (2 W/cm^2) irradiation. (c) Photothermal curves of HSZGO aqueous solutions (1 mg/mL) in the presence of NaHS (5 mM) under different powers of 808nm laser. (d) Photothermal curves of HSZGO aqueous solutions (1 mg/mL) in the presence of NaHS (5 mM) at different interference under 808 nm irradiation (2 W/cm^2).

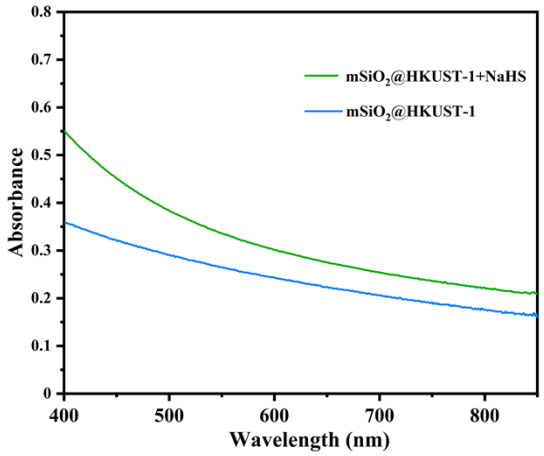

Figure S6. UV-Vis absorption spectrum of $mSiO_2$@HKUST nanoparticles and $mSiO_2$@HKUST nanoparticles (1 mg/mL) added with NaHS (5 mM).

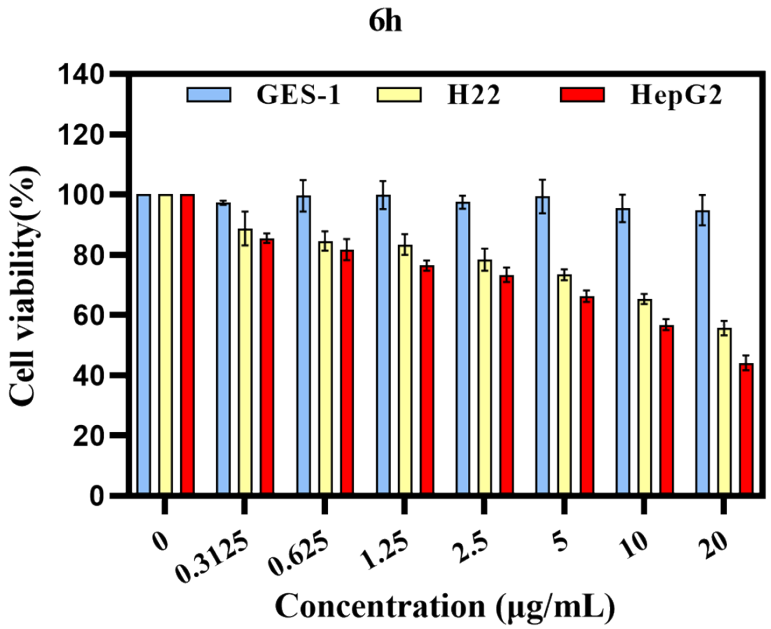

Figure S7. Cell viabilities of GES-1, H22 and HepG2 cell incubated with different concentrations of HSZGO (0, 0.3125, 0.625, 1.25, 2.5, 5, 10, 20 μg/mL) for 6 h (n=6).

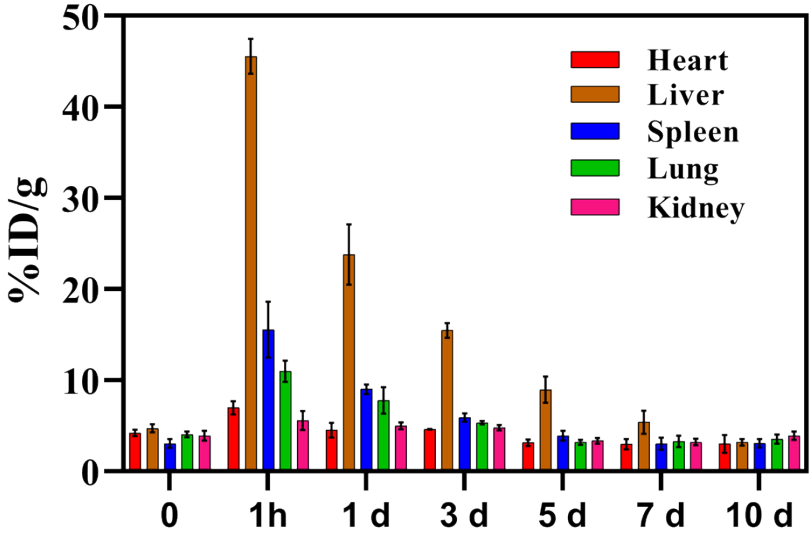

Figure S8. The biodistribution of Cu in major organs at different time (n=3).

Ⅲ. BIOSAFETY

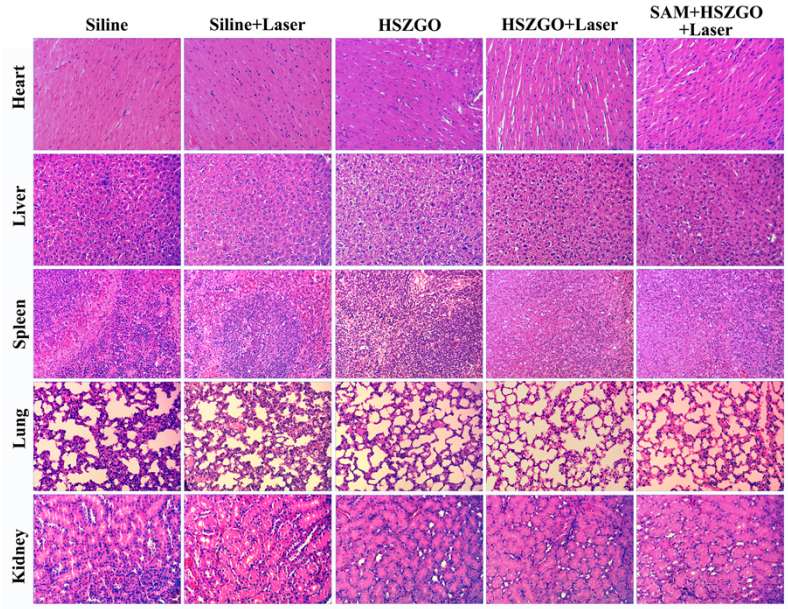

Figure S9. Representative H&E-stained tissue sections of the major organs, including the hearts, livers, spleens, lungs, and kidneys.

Ⅳ. REFERENCES

1. L. Xu and J. He, *ACS applied materials & interfaces*, 2012, **4**, 3293-3299.
2. L. Li, X. L. Liu, M. Gao, W. Hong, G. Z. Liu, L. Fan, B. Hu, Q. H. Xia, L. Liu, G. W. Song and Z. S. Xu, *J. Mater. Chem. A*, 2014, **2**, 1795-1801.
3. Q. You, K. Zhang, J. Liu, C. Liu, H. Wang, M. Wang, S. Ye, H. Gao, L. Lv, C. Wang, L. Zhu and Y. Yang, *Adv Sci (Weinh)*, 2020, **7**, 1903341.
4. L. An, X. Wang, X. Rui, J. Lin, H. Yang, Q. Tian, C. Tao and S. Yang, *Angewandte Chemie*, 2018, **57**, 15782-15786.